Fluctuations of the Impulse Rate in *Limulus* Eccentric Cells

ROBERT SHAPLEY

From The Rockefeller University, New York 10021

ABSTRACT Fluctuations in the discharge of impulses were studied in eccentric cells of the compound eye of the horseshoe crab, *Limulus polyphemus*. A theory is presented which accounts for the variability in the response of the eccentric cell to light. The main idea of this theory is that the source of randomness in the impulse rate is "noise" in the generator potential. Another essential aspect of the theory is that the process which transforms the generator potential "noise" into the impulse rate fluctuations may be treated as a linear filter. These ideas lead directly to Fourier analysis of the fluctuations. Experimental verification of theoretical predictions was obtained by calculation of the variance spectrum of the impulse rate. The variance spectrum of the impulse rate is shown to be the filtered variance spectrum of the generator potential.

INTRODUCTION

Some degree of randomness in the maintained response of a neuron to steady stimulation is characteristic of sensory neurons and neurons of vertebrate and invertebrate central nervous systems. The study of neuronal fluctuations is significant because these fluctuations are widespread, and because they may provide detailed understanding of the function of single neurons (Burns, 1968).

Numerous investigators have studied fluctuations of the maintained response of primary sensory neurons—cells which do not receive convergent input from other neurons (frog muscle spindle [Buller et al., 1953]; *Limulus* visual cells [Ratliff et al., 1968]; cat auditory nerve [Kiang, 1965]; mammalian cutaneous mechanoreceptors [Werner and Mountcastle, 1965]; cat muscle spindle [Stein and Matthews, 1965]; cat chemoreceptors [Biscoe and Taylor, 1962]). The sources of variability in primary sensory cells may not be the same, in detail, as those causing variability in the firing of neurons in the central nervous system. However, because the former are more susceptible to experimental control, they are more suitable for quantitative study than the richly interconnected central neurons.

I have studied the way in which randomness arises in the maintained response to light of eccentric cells in the compound eye of the horseshoe crab.

The axons of the eccentric cells gather to form the optic nerve of the horseshoe crab. As far as we know, these are the only cells in the compound eye which respond to light by firing nerve impulses (Waterman and Wiersma, 1954; Purple, 1964; Behrens and Wulff, 1965). This paper deals with fluctuations due to processes within single eccentric cells. An accompanying paper is concerned with the effect of interactions between eccentric cells.

Ratliff et al. (1968), recording from *Limulus* eccentric cells, found that the variance of the steady-state firing rate in response to electrical stimulation was much smaller than the variance of the response to stimulation by light, and that in the latter case the variance depended on light intensity and light adaptation. These results implied that the randomness in the generator potential, which is probably due to randomness in photon arrival and absorption (Dodge et al., 1968), was responsible for the impulse rate fluctuations. Because the impulse-firing mechanism can be treated as a linear filter for modulated stimuli (Dodge, 1968; Knight et al., 1970), I have used the theory for the linear filtering of stochastic processes to show how fluctuations in impulse rate arise from the generator potential "noise" (Shapley, 1969).

METHODS

The Biological Preparation

This work was done on excised lateral eyes of the horseshoe crab, *Limulus polyphemus*. For intracellular recording, the eye was sliced in half with a razor blade. The slice was parallel to the long axis of the eye and perpendicular to the surface of the eye. The sliced eye formed the fourth wall of a three-sided Plexiglass chamber; it was sealed into place with beeswax. The chamber was filled with artificial seawater. For experiments on generator potentials, the impulse-firing mechanism was poisoned by adding 10^{-6} M tetrodotoxin to the seawater.

Experiments were performed with a micropipette as an intracellular electrode. Micropipettes were filled with 3 molar potassium chloride; they had a resistance of 10–20 megohms measured in seawater. Signals were passed from the micropipette probe to a unity gain negative capacitance bridge amplifier designed by J. P. Hervey. This amplifier has been described by Purple (1964).

In other experiments, nerve fiber recording was done using standard techniques. Bundles of nerve fibers were teased from the *Limulus* optic nerve with glass needles and dissected until a single active fiber was present on the recording electrode. A preamplifier (Tektronix 122) provided a gain of 1000.

Action potentials and/or slow potentials were fed to a Tektronix 502A oscilloscope. The vertical signal output from the oscilloscope was monitored on a loudspeaker. The output of the oscilloscope was also fed into a CDC 160-A digital computer in a manner described below.

Analysis was performed on steady-state responses of eccentric cells which were statistically stationary. This means that statistical parameters of the discharge did not change during the course of one response, or from one experimental run to another.

Stimulus and Stimulus Control

Two sets of stimulus conditions were established. First, different time-varying waveforms were used to modulate the light intensity illuminating an eccentric cell or the current that was directly driving the cell. Under the second set of stimulus conditions steady stimulation was repeated at constant intervals throughout the experiment. A constant repetition rate was required because statistical measures were obtained by averaging several responses to identical steady stimuli. The responses would be statistically the same only if the cell were in the same adaptation state at the onset of each stimulus presentation.

Stimulus presentation and control were identical to those described by Knight et al. (1970). The stimulus waveform was generated by adding together constant voltages with time-varying voltages generated by a waveform generator (Hewlett-Packard 3300A). For stimulation by modulated current the summed voltage was led directly to the bridge stimulus input of the bridge amplifier. For stimulation by modulated light the summed voltage was first fed to a voltage-to-frequency converter with center frequency adjusted to 400 hz. In some experiments a steady light and a sinusoidal current were applied simultaneously to the same cell in order to modulate the activity of the cell around a level of excitation produced by the natural stimulus. For such experiments a constant voltage was passed through the voltage-to-frequency converter and the time-varying voltage was led to the bridge amplifier stimulus input and thence to the microelectrode.

The output of the voltage-to-frequency converter triggered a pulse generator (Tektronix 161) which in turn triggered a glow modulator driver. The glow modulator driver, designed by M. Rosetto, provided pulses of constant current, adjustable from 8 to 30 ma, to drive a glow modulator tube (Sylvania R1131C).

The light stimulus was brought to single ommatidia of the compound eye via fiber optics. This method is described by R. Barlow (1969).

A programmed timer was used to control the timing of experimental runs and provide electronic gating and clock signals for on-line computer data acquisition. It was similar to the one described by Milkman and Schoenfeld (1966). The programmed timer provided an input gate signal to alert the computer, and provided the 5 kc clock rate the computer used in the data acquisition program. Seven additional programmable gates were available in the programmed timer to turn stimuli on and off in a prescribed sequence.

Data Processing

The data acquisition program, written for the CDC 160A computer by H. K. Hartline, Norman Milkman, and David Lange, performed three functions which were particularly important for my experiments. First, the program measured time between pulse events on three separate data channels. Second, it sampled one voltage channel by means of an analogue to digital converter and stored the values of the voltage in memory. These two functions performed on-line took, on the average, a little less than 0.2 msec. Third, at the end of each experimental run the program stored time interval data and voltage data on magnetic tape for later analysis.

The resolution of the measurement of time intervals was 0.2 msec, the length of the clock cycle. This was 1 % accuracy for a firing rate of 50 impulses/sec, one-half % accuracy for 25 impulses/sec.

ANALYTICAL METHODS

Impulse Rate

The primary data for the experiments on impulse firing are intervals between impulses. One way to study the characteristics of neuronal discharge is to convert the list of pulse intervals into a list of instantaneous impulse rate samples. As shown below, in the case of regularly firing neurons, important statistical parameters for the impulse rate are the same as for the impulse intervals. The reason for using the pulse rate, rather than interpulse interval, as a measure of neural activity is that the rate is a more direct measure of the level of excitation of the neuron than the interval.

The algorithm for constructing the impulse rate is illustrated in Fig. 1. For any particular interval between pulses, the reciprocal of the time interval, the impulse rate, is assigned to all the time between the beginning and end of the interval. In effect, in constructing the impulse rate, one is transforming a frequency modulation into an amplitude modulation.

If the instantaneous impulse rate is sampled over equispaced intervals of time, the result is a list of pulse rate samples which can be mathematically manipulated in the same way as periodically sampled continuous functions (one might expect discontinuities in the firing rate at instants when impulses are fired; discontinuities are eliminated by averaging the instantaneous rate before and after an impulse discharge, to obtain a value of the impulse rate for those bins in which an impulse has occurred). If the "sampling" bins are small enough, a negligible amount of information about the statistics of the pulse

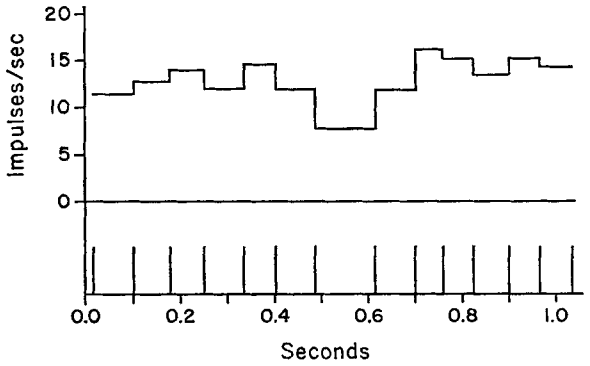

FIGURE 1. Instantaneous firing rate and the impulse train. During the interval between two pulses the impulse rate equals the reciprocal of that interval. The pulse train and impulse rate are plotted on the same time scale.

train will be lost. To be fine enough the sampling interval ought to be less than half the length of the average interspike interval, a limit consistent with the sampling theorem (see Shannon and Weaver, 1949, p. 53, for a discussion of the sampling theorem).

For the purposes of this paper, I have introduced a new unit to replace "impulses per second." This has been done in order to clarify the conception of modulation frequency of the impulse rate, which arises in the Fourier analysis of neuronal firing. The unit is named after E. D. Adrian, who discovered neural pulse frequency coding. 1 adrian equals one impulse/sec. I have used this unit in some of my figures, principally those illustrating spectral analysis of the impulse rate.

SPECTRAL ANALYSIS

Spectral analysis is an analytical tool developed to help understanding of the filtering of signals by linear, time-invariant devices. It has been applied in communication theory to the problem of filtering of stochastic processes (Parzen, 1962; Blackman and Tukey, 1958; Jenkins and Watts, 1968). I used spectral analysis to characterize the fluctuations in the impulse rate and generator potential.

Sinusoidal signals are unchanged in shape, but may be changed in amplitude and shifted in phase, when they are passed through a time-invariant linear filter (Parzen, 1962). Given any time-invariant linear filter, one can characterize it by specifying the response to a unit amplitude sinusoidal signal at each frequency. The function which relates the amplitude and phase of the output to the modulation frequency is called the frequency response.

Also, it is possible to express any continuous, deterministic function of time as a weighted sum of sinusoidal functions of time. The function which relates the relative weighting of each Fourier component to frequency is the Fourier transform of the original function. The operation of a filter on an input function can be expressed as the separate multiplication of each of the Fourier components belonging to the input function by the appropriate value of the frequency response.

For random processes a similar theory can be developed (cf. Bartlett, 1955; Parzen, 1962). A stochastic process is an ensemble of time functions which have some average properties in common but which cannot be determined exactly as a function of time. In an experimental context, this ensemble is composed of the group of noisy records which are measurements of the stochastic process.

One average property of a stochastic process is its autocovariance. The autocovariance is defined as the average product of the deviation of a random variable from its mean, multiplied by the value of the deviation later in time. For the stochastic process $n(t)$ with mean value $\bar{n}$, the autocovariance is defined as $\overline{(n(t) - \bar{n})(n(t + \tau) - \bar{n})}$. The autocovariance is a continuous, deterministic function of time; it depends on the time lag, τ, the lag between the two random variables in the product. The autocovariance is a measure of how rapidly the stochastic process fluctuates around its average value. The value of the autocovariance at zero time lag is the variance of the stochastic process; i.e., $\overline{(n(t) - \bar{n})^2}$.

The autocovariance of a stochastic process can be Fourier analyzed since it is a deterministic function of time. The Fourier transform of the autocovariance is what I call the variance spectrum. This name is appropriate because the value of the variance spectrum at a particular frequency represents the contribution of that frequency to the total variance of the stochastic process. Spectral analysis of stochastic processes was applied first to electrical signals for which variance means power, and so what I call the variance spectrum is more commonly referred to as the power spectrum (Rice, 1944).

The variance (power) spectrum of a stochastic process can also be calculated from direct Fourier analysis of the individual time functions which are members of the ensemble of functions which constitute the stochastic process. The squared amplitudes of the Fourier components must be averaged from many members of the ensemble to obtain the variance spectrum. It is a theorem that the variance spectrum computed in this manner is equal to the variance spectrum calculated from Fourier analysis of the autocovariance (Bartlett, 1955, pp. 159–166).

The function which relates the variance (power) spectrum of a stochastic process put into a linear filter to the spectrum of the output stochastic process is usually called the power transfer function of the filter (using my terminology it ought to be called the variance transfer function). It is the squared absolute value of the frequency response of the filter. The variance spectrum of the output equals the variance spectrum of the input multiplied by the power transfer function.

Spectral Estimation Spectral analysis is often performed on continuous functions of time which have been sampled at equally spaced points in time (Cooley, Lewis, and Welch, 1967). This procedure generates a list of numbers which are the values of the continuous function at the sample times. One can compute the variance spectrum of this list of numbers in the following way. First, one performs a Fourier analysis of the list; this is done by digital computer with subroutines incorporating the fast Fourier transform algorithm (Cooley et al., 1967). The Fourier transform is a list of complex numbers, each number associated with a particular frequency. One calculates the amplitude, or absolute value, of each of these numbers and squares it. The resulting list, of squared amplitudes at a number of evenly spaced points in the frequency domain, is the variance (power) spectrum, of the original list representing the time function.

If the original list is from evenly spaced time samples of a stochastic process, the sample spectrum from one record is not adequate to allow accurate estimation of the spectrum of the stochastic process. One must average several independent spectral estimates from a group of realizations of the stochastic process (cf. Jenkins and Watts, 1968, for details). What this means in a neurophysiological application is that one averages spectral estimates from several experimental runs which have identical stimulus conditions. In order to obtain smooth spectral estimates for stochastic processes I used Welch's method of averaging overlapping sample spectra (Welch, 1967).

The bandwidth of the variance spectrum is set by the frequency of sampling of the continuous signal. The bandwidth is one-half the sampling frequency. In my experiments the sampling frequency was 50 hz, so the bandwidth of the spectrum was 25 hz. The lowest frequency in the spectrum and the frequency resolution are the reciprocal of the record length. The record length was 5.12 sec so that the lowest frequency and

frequency resolution were about 0.2 hz. Smoothing reduces the resolution without changing the lowest measurable frequency. The averaged sample spectra were further smoothed to give a frequency resolution of 1 hz. This was accomplished by moving average smoothing of the spectral estimates.

AUTOCORRELATION

The autocorrelation is defined as the autocovariance divided by the variance. Thus the autocorrelation is unity at zero time lag and varies with time lag, typically becoming zero as the time lag becomes large. The autocorrelation can be derived from the variance spectrum and is an equivalent measure of the average temporal pattern of a stochastic process.

The autocorrelation of the impulse rate has a very definite relationship to the serial correlation coefficients of the impulse intervals. The autocorrelation of the impulse rate, $n(t)$, is $\overline{(n(t) - \bar{n})(n(t + \tau) - \bar{n})(n(t) - \bar{n})^2}$.

The impulse rate, n, and pulse interval, s, are related by the equation $n = \frac{1}{s}$. In fairly regularly firing nerve cells, where deviations from the mean are not large, for deviations from the mean in pulse rate $\Delta n = n(t) - \bar{n}$ and for deviations in pulse

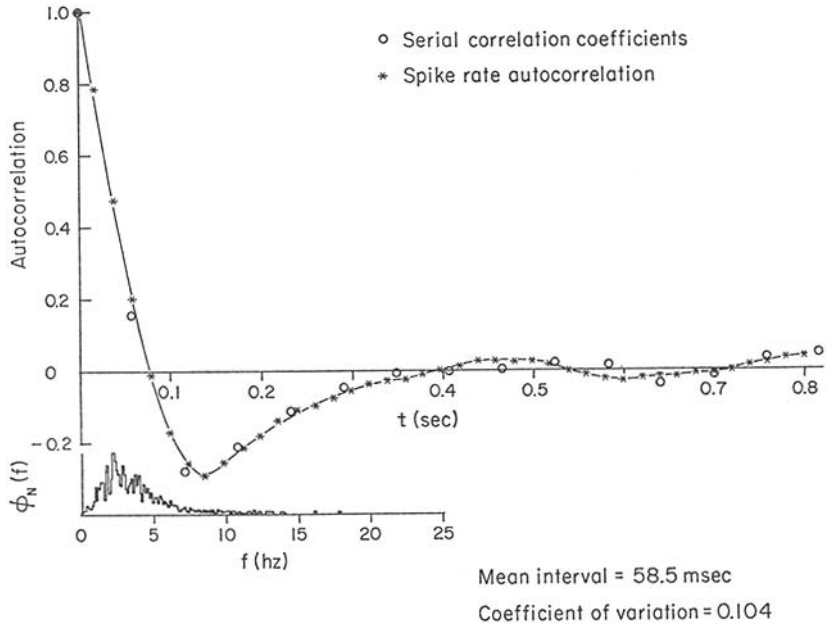

FIGURE 2. Autocorrelation of the impulse rate and serial correlation coefficients of pulse intervals. The autocorrelation is plotted as a continuous curve and as asterisks. The serial correlation coefficients are plotted as open circles at times equal to integral multiples of the mean interpulse interval. At the lower left is shown the variance spectrum of the impulse rate, from which the autocorrelation of the impulse rate was calculated by Fourier transformation.

intervals Δs, we can write $\Delta n/\bar{n} = -\Delta s/\bar{s}$. In particular, for the coefficient of variation, $\sigma_N/\bar{n} = \sigma_s/\bar{s}$. Using the same argument you can show that $r_m = \overline{\Delta S_k \Delta S_{k+m}/\Delta S_k^2} = \overline{\Delta n(t)\Delta n(t+\tau)}/\overline{\Delta n(t)^2}$ when $\tau = m\bar{s}$, where $\bar{s}$ is the mean pulse interval, r_m is the mth serial correlation coefficient, and $m = 1, 2, 3 \cdots$. In words, the autocorrelation of the impulse rate equals the interval serial correlation coefficients at time lags which equal an appropriate integral multiple of the mean interval. For example, the autocorrelation of the firing rate at time lag $\tau = 2\bar{s}$ equals the second interval serial correlation coefficient.

This is shown for some electronically generated data in Fig. 2.

This means that we can calculate the serial correlation coefficients of the intervals from the variance spectrum of the impulse rate.

RESULTS

Frequency Response of the Current-to-Firing Rate Process

The essential problem of this paper is the relation between noise in the membrane potential and variability of the impulse rate. The important mechanism to understand, in connection with this problem, is the process which produces the impulse rate from depolarization. Knight et al. (1970) have shown that this process acts like a linear transducer for small modulated signals; in other words, it can be characterized by its frequency response, $S(f)$. $S(f)$ is defined as the relative modulation (peak to peak divided by the average) of the impulse rate divided by the relative modulation of the driving current at the frequency f.

If the fluctuations in the impulse rate are due solely to filtered generator potential fluctuations, and there is no significant extra source of variability in impulse firing, we would predict,

$$\varphi_N(f) = |S(f)|^2 \cdot \varphi_G(f) \qquad (1)$$

where $\varphi_G(f)$ is the variance spectrum of the generator potential and $\varphi_N(f)$ is the variance spectrum of the impulse rate. Equation (1) is a consequence of the theory for linear filtering of noise (see Analytical Methods).

Equation (1) is correct if φ_N and φ_G are in the same units. φ_G is expressed in the units of millivolts^2/hertz (mv^2/hz). φ_N is expressed in the units adrian^2/hz; an adrian has been previously defined as 1 impulse/sec. A scale factor with units (adrian/mv)^2 must be used to convert φ_G from the units of a voltage spectrum to the units of an impulse rate spectrum. This factor was measured as the slope of the steady-state voltage vs. firing rate curve; it lay in the range 1–25 (adrian/mv)^2 (cf. Fuortes, 1959).

Observations on Filtering of Generator Potential "Noise"

In order to verify this prediction one had to measure, in each eccentric cell, the variance spectrum of the generator potential, $\varphi_G(f)$, the frequency response

of the current-to-firing rate process, $S(f)$, and the variance spectrum of the impulse rate, $\varphi_N(f)$.

The shape of a typical $S(f)$ is shown in Fig. 3 (techniques for measurement of $S(f)$ are described in detail in Knight et al., 1970). The logarithms of amplitude and phase are the ordinates and the logarithm of frequency is the abscissa in this graph. The first lobe of the phase shift is a phase lead; at frequencies above 1.5 hz the phase shift changes into a phase lag. The smooth curve

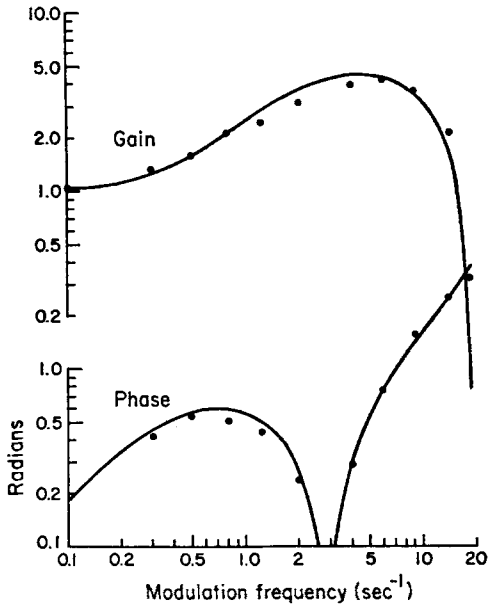

FIGURE 3. Frequency response of the current-to-firing rate mechanism. The amplitude (gain) and phase of the response to a whole range of modulated current stimuli are plotted against frequency of modulation. The points are empirical; the smooth curve is a fit to the points using Knight's (1969) theoretical expression for $S(f)$. The mean impulse rate for this cell was 20 impulses/sec.

drawn through the experimental points is the analytic expression for $S(f)$ derived by Knight (1969) and Knight et al. (1970).[1] The features of the predicted and measured frequency response are a low frequency cutoff, peak in amplitude (gain) at 5 hz, and a high frequency cutoff with a null at the frequency equal to the average impulse rate.

Spectra for both the generator potential, φ_G, and for the impulse rate, φ_N, were both measured in the same cell. Data from such an experiment are shown in Fig. 4. At the upper left is a graph of φ_G, the variance spectrum of the generator potential. Note that in this cell at this light intensity the generator

[1] This analytic expression was fit to the data by the choice of two parameters, the self-inhibitory time constant and self-inhibitory coefficient. The time constant was almost always 0.5 sec while the coefficient, which measured the magnitude of self-inhibition, had values from 2 to 5.

potential spectrum shows little peaking. Below is the predicted impulse rate variance spectrum, φ_N^*. The predicted spectrum is obtained by multiplying each value of the variance spectrum of the generator potential by its appropriate weighting factor—the squared amplitude of $S(f)$ measured in the same cell. The features introduced by filtering are apparent in the figure. The variance spectrum, φ_N^*, is peaked, with a low frequency and high frequency cutoff on either side of the peak.

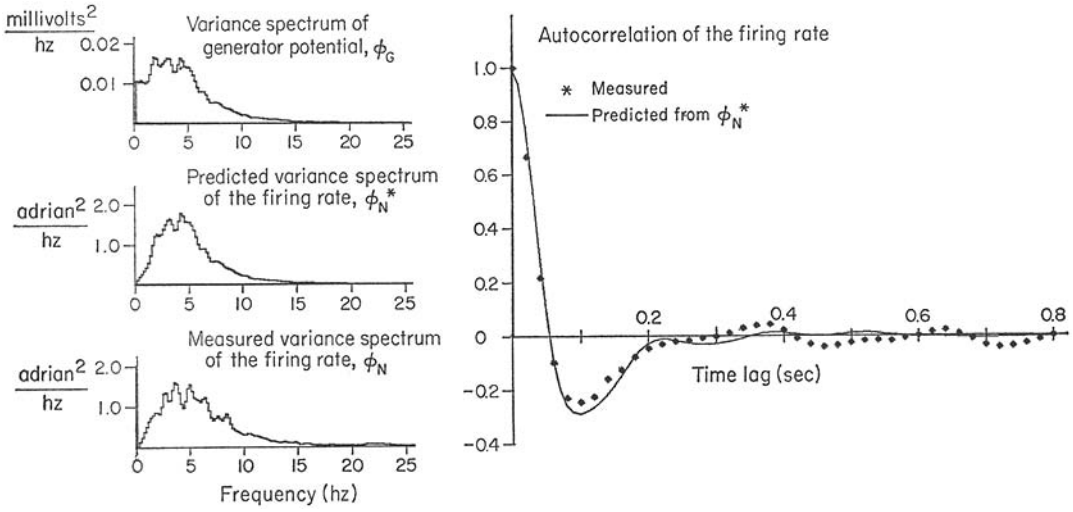

FIGURE 4. Prediction and measurement of the variance spectrum of the impulse rate. Shown in the left column are φ_G and φ_N, the measured generator potential and impulse rate variance spectra. Between them is φ_N^*, the predicted spectrum, obtained by multiplying φ_G by $|S(f)|^2$. The autocorrelations, predicted and measured, are shown at the right. The average rate was 23 impulses/sec.

The measured variance spectrum of the impulse rate, φ_N, is shown at the bottom left of Fig. 4. It appears to have almost exactly the same shape and magnitude as the predicted spectrum, φ_N^*.

We can estimate the degree of agreement of these two spectra, φ_N and φ_N^*, by comparing the differences between them with the amount of error inherent in the calculation of spectral estimates from data. As shown in texts on spectral analysis, if a stochastic process has a Gaussian distribution function, each spectral component is a random variable with a chi-squared distribution. The number of degrees of freedom for this chi-squared distribution is set by the total amount of data and the degree of frequency resolution in the spectrum (see Jenkins and Watts, 1968; Welch, 1967). When this distribution of the spectral components is used, one can calculate a standard error for the variance spectrum. In this experiment 15 estimates were averaged and were smoothed to reduce the standard error by half. This results in an approximate

standard error of 10% of the magnitude of the spectral component (the standard error is a constant fraction of the size of the spectral component—the larger the component, the larger the absolute magnitude of the standard error). The predicted and measured variance spectra, φ_N^* and φ_N, agree within 2 SE, over most of the frequency range.

The agreement of the measured variance spectrum of the impulse rate with the predicted spectrum confirms the working hypothesis with which we began. The temporal pattern of variability in the impulse rate originates in the generator potential "noise" and is filtered and therefore shaped by the impulse-firing mechanism.

PREDICTED AND MEASURED AUTOCORRELATION The autocorrelation of the impulse rate for measured data agrees well with the predicted autocorrelation which is calculated from φ_N^*. The two autocorrelation functions, measured and predicted, are shown on the right side of Fig. 4. As shown in the section on Analytical Methods, the autocorrelation of the impulse rate can be calculated from the variance spectrum. It measures in the time domain what the spectrum measures in the frequency domain—the temporal texture of a random process. Since the variance spectra, φ_N and φ_N^*, agree within the inherent error of spectral estimation, it is no accident that the predicted and measured autocorrelation functions also correspond very closely to one another.

It is clear from Fig. 4 that the current-to-firing rate mechanism strongly affects the shape of the variance spectrum. The impulse rate spectrum is far more peaked than the variance spectrum of the generator potential. The filtering of the generator potential also changes the relative amount of variability in the impulse rate; i.e., the size of the coefficient of variation.

The shape of the frequency response, $S(f)$, causes the coefficient of variation of the impulse rate to be greater than the coefficient of variation of the generator potential. Since middle range frequencies are amplified relative to constant or very low frequency stimuli, $S(f)$ is larger than 1 over most of the frequency range where the variance spectrum of the generator potential has large values (cf. Fig. 4). This results in enhancement of the fluctuations relative to the mean—in other words, a higher coefficient of variation for the impulse rate than for the generator potential.

Steady-State Fluctuations and the Frequency Response

Dodge et al. (1968) found that for steady-state fluctuations of the generator potential

$$\varphi_G(f) = \alpha \mid G(f) \mid^2 \qquad (2)$$

where $G(f)$ is the frequency response for the transduction, light to generator potential. Also, Knight et al. (1970) showed that $N(f) = S(f)\ G(f)$, where

$N(f)$ is the frequency response of the transduction from light to impulse rate. With the use of these findings and equation 1, we can derive

$$\varphi_N(f) = \beta \mid N(f) \mid^2 \tag{3}$$

The proportionality between variance spectrum and squared frequency response should be carried over to the impulse rate from the generator potential. The results of an experiment which tests this prediction are shown in Fig. 5.

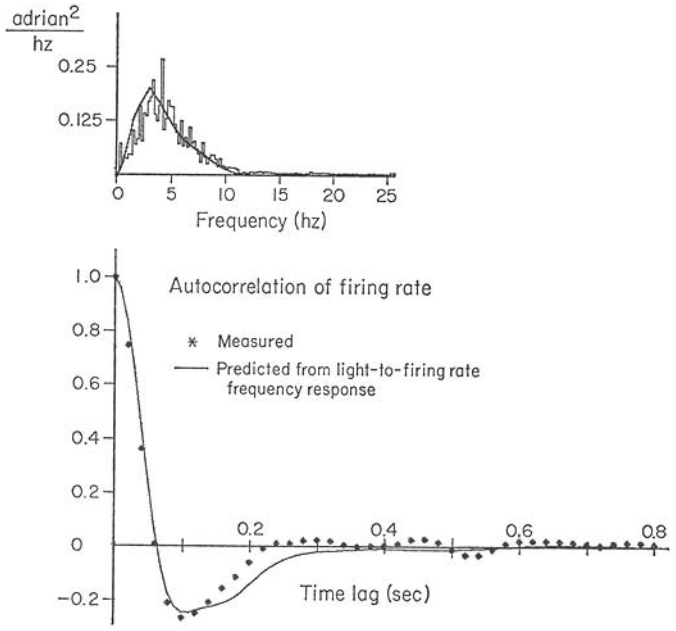

FIGURE 5. Comparison of variance spectrum with the light-to-impulse rate frequency response $N(f)$. This experiment was done with optical stimulation of a single eccentric cell with a small spot of light, steady to measure φ_N and modulated to measure $N(f)$. In the upper graph the jagged curve is φ_N and the smooth curve is $\mid N \mid^2 . \mid N(f) \mid^2$ is plotted on a vertical scale such that the area under the curve will equal the area under the variance spectrum (the variance). Autocorrelations are shown below.

Probability Densities

Probability density functions for the impulse rate under conditions of steady stimulation by light are well fit by Gaussian functions. This finding is important because the distribution of membrane potential deviations is also Gaussian under the same stimulus conditions.

Fig. 6 shows an impulse rate histogram (estimate of probability density function) and a generator potential histogram for the response to a light whose intensity was 1000 times brighter than the threshold intensity for

maintained impulse firing. Both these histograms approximate Gaussian functions; their skewness is close to zero, their kurtosis (fourth moment/variance squared) is close to three. The interval distribution is positively skewed when the impulse rate has a Gaussian distribution, as one would expect (Shapley, 1970).

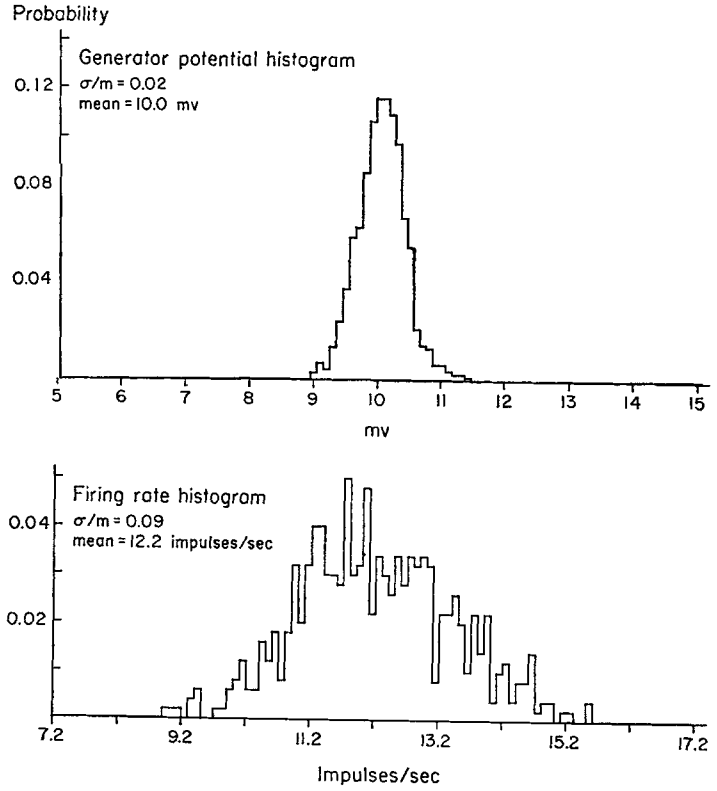

FIGURE 6. Generator potential and impulse rate histograms for the response to steady light. Both responses were recorded from cells stimulated by light intensity 100 to 1000 times brighter than the threshold for maintained discharge. Bin width for the generator potential is 0.1 mv, for the impulse rate 0.1 impulse/sec.

A marked effect occurred in the statistics of a cell stimulated by electric current, which was allowed to dark adapt for over 10 min. The statistics of the impulse rate histogram changed very greatly during dark adaptation, an effect which very convincingly reinforces the view that fluctuations in membrane potential cause the observed variability in impulse firing.

When the cell was light-adapted the membrane potential fluctuations in the dark were very small and symmetrical about the resting potential; under the same conditions the impulse rate histogram was symmetric and approximately Gaussian in shape. The source of the small variability in the firing of

a light-adapted, current-driven eccentric cell has not been investigated. I mention the statistical characteristics of the small variability under these experimental conditions to contrast them with the marked changes which occur during dark adaptation.

During dark adaptation, the striking effect which occurs is an increase in the variance of the impulse rate (previously observed by Ratliff et al., 1968), and a marked increase in the skewness of the impulse rate distribution. Under the same conditions of dark adaptation, it is well-known that the membrane potential distribution changes its character, because of the low rate of appearance of large, discrete slow potentials (Yeandle, 1957; Adolph, 1964). These discrete events were occurring at the rate of 2/sec in the eccentric cell whose impulse rate distribution is graphed in Fig. 7. The distribution of the membrane potential in an eccentric cell under the same conditions of dark adapta-

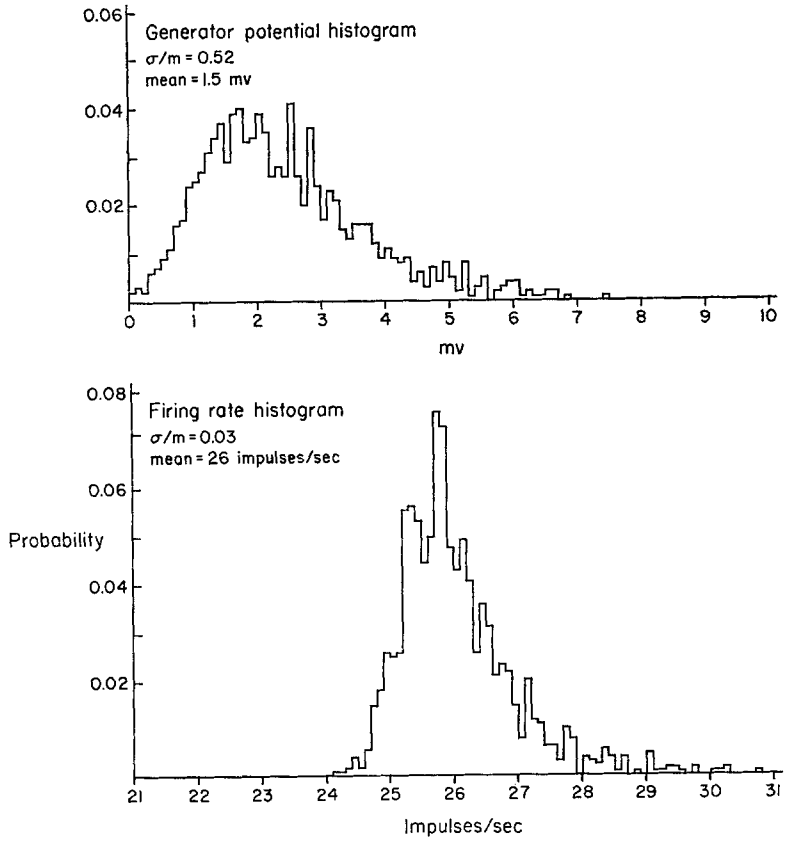

FIGURE 7. Membrane potential and impulse rate histograms for a dark-adapted cell driven by steady current. This figure demonstrates the skewness of the membrane potential and impulse rate in a thoroughly dark-adapted cell. The skewness results from the slow rate of discrete slow potentials which tend to depolarize the cell.

tion is shown in the upper graph of Fig. 7. The skewness of the membrane potential is very obvious. The values of the parameter of skewness, the ratio third moment squared divided by variance cubed, for the histograms of membrane potential and impulse rate, are both about 2.5. This is very significantly different from the value of zero expected for a symmetrical distribution. Both the membrane potential distribution and the impulse rate distribution are positively skewed; the impulse interval distribution is markedly negatively skewed under these conditions.

This large increase in skewness during dark adaptation in the probability density functions of both the membrane potential and impulse rate reinforces even more the idea that random fluctuations in membrane potential underlie the major portion of variability in the impulse rate.

DISCUSSION

The preceding results confirm the hypothesis that membrane potential "noise" causes the variability of the impulse rate. The amount of variability in the response to light, and its temporal pattern, result from the filtering of the generator potential by the current-to-firing rate mechanism.

The current-to-firing rate process is composed of two separate mechanisms—an integration mechanism and self-inhibition (Knight et al., 1970). These two mechanisms account for the shape of $S(f)$, the frequency response for the current-to-firing rate transduction, and therefore they help to shape the variance spectrum of the impulse rate.

The transformation of depolarization into impulse rate is accurately described by an integrate-and-fire model (Knight et al., 1970). In this model, membrane potential (or current through the membrane) is integrated until the integral reaches a threshold and then an impulse is fired and the integral is reset to zero.

There is also a stage of negative feedback or self-inhibition in the *Limulus* eccentric cell (Stevens, 1964; Knight et al., 1970). Purple (1964) showed that each nerve impulse in an eccentric cell triggers a long-lasting hyperpolarization, accompanied by an increase in the conductance of the membrane. The time course of the hyperpolarization is a decaying exponential with a time constant of about half a second.

Self-inhibition is the source of the low frequency cutoff in $S(f)$, and consequently in $\varphi_N(f)$. In other words, self-inhibition causes the negative correlation in the autocorrelation of the impulse rate (see Figs. 4 and 5). Similar persistent negative correlations have been noticed by other investigators working on different neurons; e.g., the work of Geisler and Goldberg (1966) on cells in the superior olivary complex of the cat. As I have already implied, a negative feedback like self-inhibition also has the effect of increasing the coef-

ficient of variation of the impulse rate by inhibiting the DC component of the underlying generator potential more than it inhibits the fluctuations.

While self-inhibition and temporal integration affect the shape of $\varphi_N(f)$, the main determinant of the magnitude and bandwidth of $\varphi_N(f)$ is the generator potential "noise," as characterized by $\varphi_G(f)$ (see Fig. 4).

The generator potential, a depolarization induced by light, appears to be quantized, as if each effectively absorbed photon triggered a unit slow potential fluctuation. The occurrence of the discrete potentials is a random process, presumably reflecting the randomness in the arrival and absorption of photons. The generator potential is therefore the summation of randomly occurring, similarly shaped discrete events. Consequently, at all light intensities, the generator potential has an inherent noisy component (Dodge et al., 1968).

These discrete slow potentials adapt with light intensity, becoming smaller and briefer at higher light intensities (Yeandle, 1957; Adolph, 1964; Dodge et al., 1968). Dodge et al. (1968) showed that the characteristics of the generator potential at all light intensities, its frequency response and variance spectrum, $\varphi_G(f)$, could be accounted for by the summation of the discrete potentials. The effect of intensity on $\varphi_N(f)$ is roughly commensurate with its effect on $\varphi_G(f)$. Thus, diminution of quantal responses at higher light intensities results in a lower coefficient of variation of the impulse rate. An analogous effect should be observed in other neurons; i.e., reduction in the coefficient of variation of the impulse rate whenever there is adaptation in the size of excitatory synaptic potentials. Synaptic "adaptation" might be caused by fatigue, or by presynaptic inhibition. The effect of adaptation on variability of impulse discharge has already been shown by Stein (1967) for a general neuron model and inferred by H. B. Barlow and Levick (1969) from a mathematical model for mammalian retinal ganglion cells.

Finally, my direct measurements of the underlying processes which cause neuronal variability support some of the theoretical speculations of others. In particular, they reinforce the conjectures of Walløe (1968) and Matthews and Stein (1969), that the pattern of the interval serial correlation coefficients should be related to underlying periodicities in the membrane potential.

I am very grateful to Frederick Dodge, Bruce Knight, Floyd Ratliff, and H.K. Hartline for their help and encouragement. This work formed part of a dissertation submitted to The Rockefeller University in fulfillment of the requirements for a Ph.D. degree.

This work was supported by grant B 864 from the National Institute of Neurological Diseases and Blindness, grant GB 654 OX from the National Science Foundation, and by a National Science Foundation Graduate Fellowship.

Received for publication 20 August 1970.

REFERENCES

ADOLPH, A. 1964. Spontaneous slow potential fluctuations in the *Limulus* photoreceptor. *J. Gen. Physiol.* **48**:297.

BARLOW, H. B., and W. R. LEVICK. 1969. Changes in the maintained discharge with adaptation level in the cat retina. *J. Physiol. (London).* **202**:699.

BARLOW, R. 1969. Inhibitory fields in the *Limulus* lateral eye. *J. Gen. Physiol.* **54**:383.

BARTLETT, M. S. 1955. An Introduction to Stochastic Processes. Cambridge University Press, Cambridge.

BEHRENS, M. E., and V. J. WULFF. 1965. Light-initiated responses of retinula and eccentric cells in the *Limulus* lateral eye. *J. Gen. Physiol.* **48**:1081.

BISCOE, T. J., and A. TAYLOR. 1962. Irregularity of discharge of carotid body chemoreceptors. *J. Physiol. (London).* **163**:4P.

BLACKMAN, R. B., and J. W. TUKEY. 1958. The Measurement of Power Spectra. Dover Publications, Inc., New York.

BULLER, A., J. NICHOLLS, and G. STRÖM. 1953. Spontaneous fluctuation in excitability in the muscle spindle of the frog. *J. Physiol. (London).* **122**:409.

BURNS, B. D. 1968. The Uncertain Nervous System. Edward Arnold (Publishers) Ltd., London.

COOLEY, J. W., P. A. W. LEWIS, and P. D. WELCH. 1967. Historical notes on the fast Fourier transform. *IEEE Trans. Audio Electroacoustics.* **AU-15**:76.

DODGE, F. A. 1968. Excitation and inhibition in the eye of *Limulus*. *In* Optical Data Processing by Organisms and Machines. W. REICHARDT, Academic Press, Inc., New York.

DODGE, F. A., B. W. KNIGHT, and J. TOYODA. 1968. Voltage noise in *Limulus* visual cells. *Science (Washington).* **160**:88.

FUORTES, M. G. F. 1959. Initiation of impulses in visual cells. *J. Physiol. (London).* **148**:14.

GEISLER, C., and J. GOLDBERG. 1966. A stochastic model of the repetitive activity of neurons. *Biophys. J.* **6**:53.

JENKINS, G., and D. WATTS. 1968. Spectral Analysis and Its Applications. Holden-Day, Inc., San Francisco.

KIANG, N. 1965. Discharge Patterns of Single Fibers in the Cat's Auditory Nerve. Massachusetts Institute of Technology Press, Cambridge, Mass.

KNIGHT, B. 1969. Frequency response for sampling integrator and for voltage to frequency converter. *In* Systems Analysis in Neurophysiology (notes from a conference held at Brainerd, Minn. C. Terzuolo, editor).

KNIGHT, B., J. TOYODA, and F. A. DODGE. 1970. A quantitative description of the dynamics of excitation and inhibition in the eye of *Limulus*. *J. Gen. Physiol.* **56**:421.

MATTHEWS, P. B. C., and R. B. STEIN. 1969. The regularity of primary and secondary muscle spindle afferent discharges. *J. Physiol. (London).* **202**:59.

MILKMAN, N., and R. SCHOENFELD. 1966. A digital programmer for stimuli and computer control in physiological experiments. *Ann. N. Y. Acad. Sci.* **128**:861.

PARZEN, E. 1962. Stochastic Processes. Holden-Day, Inc., San Francisco.

PURPLE, R. 1964. The Integration of Excitatory and Inhibitory Influences in the Eccentric Cell of the Eye of *Limulus*. Ph.D. Thesis. The Rockefeller University, New York.

RATLIFF, F., H. K. HARTLINE, and D. LANGE. 1968. Variability of interspike intervals in optic nerve fibers of *Limulus*: Effect of light and dark adaptation. *Proc. Nat. Acad. Sci. U.S.A.* **60**:392.

RICE, S. O. 1944. Mathematical analysis of random noise. *Bell Teleph. Syst. J.* **23**:282.

SHANNON, C. E., and W. WEAVER. 1949. The Mathematical Theory of Communication. University of Illinois Press, Urbana, Ill.

SHAPLEY, R. 1969. Fluctuations in the response to light of visual neurons in *Limulus*. *Nature (London).* **221**:437.

SHAPLEY, R. 1970. Variability of Impulse Firing in Eccentric Cells of the *Limulus* Eye. Ph.D. Thesis. The Rockefeller University. New York.

STEIN, R. 1967. Some models of neuronal variability. *Biophys. J.* **7**:37.

STEIN, R., and P. B. C. MATTHEWS. 1965. Differences in variability of discharge frequency between primary and secondary muscle spindle afferent endings of the cat. *Nature (London).* **208**:1217.

STEVENS, C. 1964. A Quantitative Theory of Neural Interaction: Theoretical and Experimental Investigations. Ph.D. Thesis. The Rockefeller University, New York.

WALLØE, L. 1968. Transfer of Signals through a Second Order Sensory Neuron. Ph.D. Thesis. University of Oslo, Oslo.

WATERMAN, T. H., and C. A. G. WIERSMA. 1954. The functional relation between retinal cells and optic nerve in *Limulus*. *J. Exp. Zool.* **126**:59.

WELCH, P. D. 1967. The use of fast Fourier transform for the estimation of power spectra: A method based on time averaging over short, modified periodograms. *IEEE Trans. Audio Electroacoustics.* **AU-15**:70.

WERNER, G., and V. MOUNTCASTLE. 1965. Neural activity in mechanoreceptive cutaneous afferents: Stimulus response relations, Weber functions, and information transmission. *J. Neurophysiol.* **28**:359.

YEANDLE, S. 1957: Studies on the Slow Potential and the Effects of Cations on the Electrical Responses of the *Limulus* Ommatidium (with an Appendix on the Quantal Nature of the Slow Potential). Ph.D. Thesis. The Johns Hopkins University, Baltimore.